



Pre-monsoon lightning in Bangladesh: Separating most from least active days with thermodynamic and synoptic composites

M. Rafiuddin^a, Nasreen Akter^a, Ashraf Dewan^{b,*}, Mohammed Sarfaraz Gani Adnan^c, Ronald L. Holle^d

^a Department of Physics, Bangladesh University of Engineering & Technology, Dhaka 1000, Bangladesh

^b Spatial Sciences Discipline, School of Earth and Planetary Sciences, Curtin University, Kent Street, Bentley, Perth, WA 6012, Australia

^c Department of Civil and Environmental Engineering, Brunel University of London, Uxbridge UB8 3PH, United Kingdom

^d Holle Meteorology and Photography, Oro Valley, AZ, United States

ARTICLE INFO

Keywords:

Pre-monsoon lightning
Thermodynamics indices
Synoptic composites
Threshold value
Bangladesh

ABSTRACT

The pre-monsoon season (March–May) in Bangladesh is the most hazardous period for lightning-related human casualties, particularly during morning and afternoon hours. This heightened risk is primarily associated with labor-intensive manual agriculture on smallholder farms. This study investigates the atmospheric conditions corresponding to the 50 most active and 50 least active pre-monsoon lightning days between 2015 and 2020. Analysis of sounding and reanalysis data reveals distinct differences across nearly all dynamic, thermodynamic, surface, and upper-air composite parameters. On the most active lightning days, the environment typically features a SWEAT index exceeding 230, a mixed-layer mixing ratio above 15 g kg^{-1} , and high values of the most unstable convective available potential energy ($\geq 1580 \text{ J kg}^{-1}$), along with elevated instability—all conducive to thunderstorms with heavy rainfall. Notably, on 20 % of these active days, storm-relative environmental helicity reaches between 300 and $485 \text{ m}^2 \text{ s}^{-2}$, indicating a high potential for supercell thunderstorms and intense lightning activity. In contrast, the least-active lightning days are characterized by weaker storm systems. These variations are primarily driven by strong, warm, moist southwesterly winds from the Bay of Bengal, which enhance horizontal temperature gradients and atmospheric instability. Regression models identified potential instability, cloud ice water content, and cloud liquid water content as strong synoptic-scale predictors of lightning activity. Principal component analysis (PCA) further highlighted the critical role of cloud-scale thermodynamic and kinematic variables in distinguishing lightning intensity. These findings provide a foundation for developing daily lightning forecast systems, with potential benefits for public safety and protection of lightning-sensitive infrastructure.

1. Introduction

Lightning occurs more frequently in the continental tropics than in most other parts of the world (Cooper and Holle, 2019). Many developing countries in tropical regions, such as Bangladesh, have large portions of the population working outdoors in labor-intensive agriculture and living or working in structures without adequate lightning protection, making them highly vulnerable. However, data collection in such regions is often limited due to resource constraints, lack of trained personnel, and the absence of centralized national databases. As a result, it is challenging to find multi-year national datasets on lightning fatalities in the tropics (Holle, 2016). Nevertheless, the government of

Bangladesh has acknowledged the seriousness of the issue and officially classified lightning as a hazard, alongside floods, tropical cyclones, and other natural hazards (MoDMR, 2019).

Using data from the Optical Transient Detector (OTD), Lightning Imaging Sensor (LIS), and ground-based lightning detection sensors, many studies have quantified lightning activity at various spatial and temporal scales (Chandra et al., 2021; Albrecht et al., 2016; Dai et al., 2009; Christian et al., 2003), thereby enhancing our understanding of this localized atmospheric phenomenon. For example, Albrecht et al. (2016) and Christian et al. (2003) demonstrated significant global variation in lightning occurrence, showing that land areas experience more lightning than oceans. They also identified the Indian subcontinent

* Corresponding author.

E-mail address: A.Dewan@curtin.edu.au (A. Dewan).

<https://doi.org/10.1016/j.atmosres.2025.108261>

Received 2 December 2024; Received in revised form 4 May 2025; Accepted 28 May 2025

Available online 31 May 2025

0169-8095/© 2025 The Author(s). Published by Elsevier B.V. This is an open access article under the CC BY license (<http://creativecommons.org/licenses/by/4.0/>).

as one of the lightning hotspots on Earth, with significant implications for its largely agrarian population. In addition to global patterns, regional and local studies have explored the relationship between lightning and various surface, dynamic, and thermodynamic factors across Asia, including the Himalayan region (e.g., Kandalgaonkar et al., 2003; Siingh et al., 2013; Qie et al., 2021). Kandalgaonkar et al. (2003) noted a pronounced diurnal cycle of lightning over the Indian region, alongside strong seasonality (Dewan et al., 2017). Factors such as convective available potential energy (CAPE), surface heat flux, topography, moisture availability, and prevailing winds have been shown to influence the spatiotemporal variability of lightning in this region (Murugavel et al., 2014; Li et al., 2020; Sahu et al., 2020; Chandra et al., 2021).

Several studies have explored how different atmospheric parameters relate to lightning activity. Dewan et al. (2018), for instance, examined the relationship between lightning, precipitation, and CAPE using Tropical Rainfall Measuring Mission's (TRMM) LIS and ERA data from 1998 to 2014. They found strong seasonal correlations between lightning flashes and CAPE, total rain, and convective rain over Bangladesh, though the correlations were weaker annually. CAPE was identified as a significant indicator of lightning across the country. Yamane and Hayashi (2006) investigated environmental factors driving thunderstorms in the Indian subcontinent during the pre-monsoon season (March–May). They found that organized convection, supported by high CAPE with vertical wind shear, was more likely to cause severe storms during the pre-monsoon than in the monsoon season (June–September). Kodama et al. (2005), using three-year averages of rainfall, lightning flash counts, mean echo-top height, and 925 hPa winds over the tropical monsoon regions, showed that lightning was associated with deep convection in the pre-monsoon season, but declined significantly following the onset of the monsoon in Bangladesh. Sugimoto and Takahashi (2017) reported similar findings, suggesting that deep convective precipitation dominates during the pre-monsoon season, while stratiform and shallow convection lead to reduced lightning activity during the monsoon. Romatschke and Houze (2011) confirmed similar patterns across the Indian region. Murugavel et al. (2014) emphasized that CAPE and local meteorological conditions are critical for thunderstorm and lightning development, particularly in northeast India and neighboring areas. Additional mechanisms—such as the presence of a dry line (Weston, 1972) and abundant low-tropospheric moisture driven by prevailing westerlies—also contribute to pre-monsoon lightning (Siingh et al., 2014). Case et al. (2023) recently assessed ensemble models for South Asia, particularly the Himalayan region, highlighting their skill in forecasting severe weather in Nepal and Bangladesh one to two days in advance. They also explored the relationships between model outputs and several meteorological variables, including lightning, rainfall, and wind.

Selected lightning events and some pre-monsoon months have been analyzed using the Lightning potential index (LPI), synoptic parameters, and atmospheric stability indices. Indices such as the Lifted index (LI), the Showalter index (SWI), CAPE, and low-pressure troughs are associated with lightning during April and May across Bangladesh (Farukh et al., 2023). While high CAPE and total precipitable water (TPW) have shown correlations with lightning activity in parts of the country, Umakanth et al. (2020) reported that the K index (KI) and Total Totals index (TTI) could help predict up to 90 % of severe thunderstorms and lightning events at the sub-divisional scale. Based on two thunderstorm cases in 2018, Paul et al. (2022) showed that high CAPE and TTI, along with elevated ice and graupel mixing ratios at cloud centers, contributed to lightning development. Five high-impact lightning events from 2019 to 2021 were modeled using two diagnostic prediction systems (WRF-ARW, WRF-ELEC), demonstrating that local ice and graupel content are effective predictors of lightning over Bangladesh (Rabbani et al., 2022). Surface characteristics such as topography (Chowdhury and De, 1995; Romatschke et al., 2010) and the existence of many water bodies (e.g., large rivers and wetlands) also play a role in driving atmospheric

instability. For example, Medina et al. (2010) showed that high daytime latent heat flux from water bodies supports the growth of convective systems across the Himalayan region. Dewan et al. (2022) found that water bodies and herbaceous wetlands are triggers of cloud-to-ground lightning between March and June in Bangladesh. Although lightning research in the country has grown recently, mainly due to the high fatalities, comprehensive studies integrating synoptic conditions, stability indices, and hydrometeors remain scarce.

Beyond the human toll, lightning has widespread global impacts. Critical infrastructures such as power utilities, wind turbines, petrochemical plants, and railway systems are particularly vulnerable to lightning in developing countries (Gomes, 2021). Lightning also contributes to forest fires (Kalashnikov et al., 2024) and poses risks to homes, sporting events (Walsh et al., 2013), and other assets, resulting in substantial protection and warning costs (Uman, 2009; Holle et al., 2016). Bangladesh has multi-decade lightning fatality data, but recent improvements in internet access and media coverage have yielded better reporting. As such, 251 deaths per year from 2010 to 2016 are considered a representative estimate of the current condition (Dewan et al., 2017). Reliable injury data, however, remain limited and are typically absent from such studies, including in Bangladesh. However, several recent investigations have provided a clearer picture of lightning-related mortality in the country. First, 79 % of annual lightning fatalities occur from March through June (Holle et al., 2019). Between 2013 and 2017, Bangladesh averaged 1.73 lightning deaths per day during the pre-monsoon season, 0.71 during the monsoon, and far fewer in other seasons (Holle et al., 2019). Second, Bangladesh exhibits a unique pattern in which lightning fatalities occur equally in the morning and afternoon, likely due to its distinct meteorological conditions—an observation not reported in any other country to date (Dewan et al., 2017; Nag et al., 2017; Holle et al., 2019). Third, the most vulnerable group comprises men engaged in manual, labor-intensive agricultural work during the pre-monsoon season (Dewan et al., 2017).

The population in Bangladesh has a high level of vulnerability to lightning, particularly during the pre-monsoon season, highlighting the need to better understand how upper-air atmospheric conditions influence this situation. This study examines the role of dynamic and thermodynamic atmospheric factors that promote active and least active lightning incidences during 2015–2020. By analyzing atmospheric variables derived from sounding and reanalysis data, we aim to identify statistically significant variables that can be used to forecast lightning in Bangladesh. This work is a step towards a real-time lightning prediction system.

2. Data and methods

2.1. Lightning data

This study used the Global Lightning Dataset, commonly referred to as GLD360. The GLD360 network utilizes a global positioning system (GPS)-synchronized broadband measurements sampled at 100 kHz, with a cutoff frequency near 48 kHz. Each receiver employs orthogonally oriented air-core loop antennas to measure the horizontal magnetic field. These sensors are capable of detecting lightning at ranges up to 10,000 km away, though the specific detection range depends on the source amplitude, direction, time of day, and geomagnetic latitude (Said et al., 2023). Virts et al. (2024) estimated the flash detection efficiency (DE) of GLD360 for 2014 and 2017–2022, demonstrating a DE ranging from 60 % to 75 %. Since GLD360 uses a combination of time-of-arrival and magnetic direction-finding techniques and requires only three sensors to determine a solution (Said et al., 2010), flash DE is relatively stable despite sensor outages and diurnal propagation effects.

For Bangladesh, the cloud-to-ground (CG) flash detection efficiency of the GLD360 network is approximately 60 % of the actual CG flash density. The data used in this study do not distinguish between CG strokes and cloud pulses, nor are they corrected for detection efficiency.

CG strokes were not grouped into CG flashes but counted individually, and for this analysis, they were treated equally to cloud strokes in tallying the total number of lightning strokes.

Due to the high sensitivity and long detection range of the sensors, lightning coverage across Bangladesh is uniform, without localized gaps or artificial maxima/minima (Said et al., 2013; Said, 2017). Lightning data were assigned to calendar days based on local standard time (LST), beginning at 00:00 and ending at 23:59 within the bounding box of Bangladesh. Previous studies by Holle et al. (2019) and Dewan et al. (2022) also utilized GLD360 data for Bangladesh, highlighting the pre-monsoon season as particularly active for lightning activity. In this study, we analyzed daily lightning stroke data from GLD360 for the pre-monsoon period (March 1 to June 15) over six years, from 2015 to 2020.

Fig. 1a shows the frequency of lightning strokes during each pre-monsoon season (107 days per year) along with the average number of strokes across the six-year period (642 days in total). Out of these 642 days, lightning was recorded on 561 days within the study area. The daily stroke counts showed substantial variability, ranging from as few as 1 to as many as 366,130 strokes. Lightning activity was typically concentrated between April and mid-June, with March exhibiting the lowest frequency. The two highest daily stroke counts occurred during the study period on 11 June 2016 and 01 June 2017, while the lowest were observed on 04 May 2015 and 17 March 2016.

To investigate atmospheric conditions associated with contrasting lightning extremes, approximately 20 % of the dataset was selected, comprising the 50 days with the highest lightning stroke counts and the 50 days with the lowest. The former are referred to as ‘active lightning days,’ and the latter as ‘least-active lightning days’ in this study. The full distribution of lightning strokes, along with the selection thresholds, is presented in Fig. 1b.

2.2. Upper air sounding data

Upper air sounding data were collected for the period from 01 March to 15 June for the years 2015 to 2020 at 00:00 UTC (06:00 LST) and 12:00 UTC (18:00 LST) for Dhaka, the capital of Bangladesh. These data were retrieved from the University of Wyoming’s online atmospheric sounding archive (<https://weather.uwyo.edu/upperair/sounding.html>). At both 00:00 and 12:00 UTC, the following thermodynamic and kinematic parameters were computed: severe weather threat (SWEAT), KI, LI, lifting condensation level (LCL), surface-based CAPE (SBCAPE), most unstable CAPE (MUCAPE), TTI, TPW, storm-relative environmental helicity (SREH), vertical wind shear (VWS), equivalent potential temperature (θ_e), and mixing ratio (Q).

Due to various operational or environmental reasons, upper air soundings were unavailable on some days. However, there was no

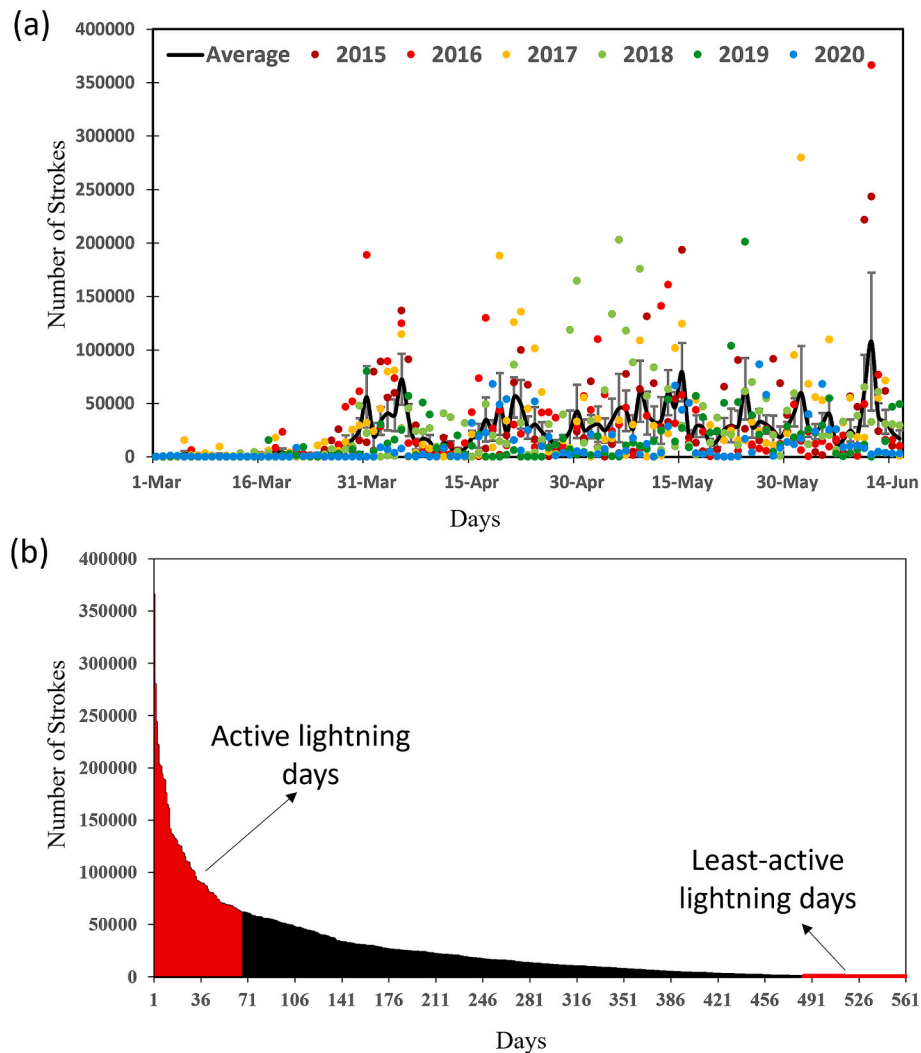


Fig. 1. (a) The number of daily strokes for each year and their averages with standard error bars; (b) Illustration of maximum to minimum lightning strokes for 561 days from 01 March to 15 June during 2015–2020. The red color in Fig. 1b indicates the studied days. (For interpretation of the references to color in this figure legend, the reader is referred to the web version of this article.)

indication of systematic bias in the data concerning high lightning activity, strong winds, or rainfall. As a result, to ensure data integrity and consistency, only the top 50 active and least-active lightning days with complete upper air sounding were included. Among the top 66 lightning days, 16 had missing sounding, leaving 50 suitable 'active' days. Similarly, from the 77 least-active days, 27 were removed due to missing sounding data, yielding 50 'least-active' days. This approach ensures comparability between the two groups (active vs least active) and facilitates a robust evaluation of the environmental differences.

It is worth noting that our method of classifying the most and least-active lightning days differs from the monsoon 'bursts and breaks' concept applied by Watson et al. (1994) in Arizona. In that study, multi-day periods with elevated or suppressed activity were used. In contrast, no consistent multi-day lightning surge pattern was identified in Bangladesh during the pre-monsoon season, and the occasional absence of soundings makes such an approach less feasible. Nevertheless, identifying daily-scale differences in upper air profiles between active and least-active lightning days remains a valuable method for understanding the causes of lightning occurrence in the region. Composites are often used to analyze regional atmospheric patterns, as demonstrated by Suriano et al. (2023) and others. Applying this approach to Bangladesh provides a meaningful way to characterize and compare atmospheric environments associated with lightning extremes.

2.3. ERA reanalysis product

For the synoptic-scale environmental analysis, data were extracted from the ERA5 reanalysis product provided by the European Centre for Medium-Range Weather Forecasts (ECMWF), with a spatial resolution of $0.25^\circ \times 0.25^\circ$ and a six-hour temporal resolution. Variables including wind, vertical velocity, θ_e , cloud ice, cloud snow, and cloud liquid water were retrieved for the region encompassing Bangladesh and its surroundings. These data were used to examine the environmental characteristics associated with various hydrometeors during active and least-active lightning days. The primary goal of this analysis was to investigate the spatial distribution of hydrometeors and evaluate related stability indices to aid in forecasting the most and the least active lightning days across Bangladesh.

2.4. Statistical models and analyses

Statistical methods such as multicollinearity diagnosis, multiple linear regression, logistic regression, and principal component analysis (PCA) are applied and analyzed with R in this study. Additionally, box-whisker plots are used to illustrate the data distribution.

2.4.1. Regression models

This study employed both multiple linear regression and logistic regression models to quantify the influence of various environmental parameters on the number of lightning strokes. The multiple linear regression models assessed the relationship between lightning stroke frequency, on both highly active and least-active lightning days, and selected environmental predictors. Before constructing the regression models, a multicollinearity diagnostic was performed to ensure that the independent variables were not excessively correlated. Multicollinearity, a statistical phenomenon occurring when two or more independent variables exhibit strong linear relationships, can distort regression results. The variance inflation factor (VIF) was calculated for each predictor to detect and assess multicollinearity. VIF measures the degree to which the variance of a regression coefficient is inflated due to multicollinearity. For a given independent variable X_i , the VIF is calculated as:

$$\text{VIF}(X_i) = \frac{1}{1 - R_i^2}$$

where R_i^2 is the coefficient of determination obtained by regressing X_i on all the other independent variables in the model. Here, $\text{VIF} = 1$: no multicollinearity; $1 < \text{VIF} < 5$: moderate correlation (usually acceptable); $\text{VIF} \geq 10$: high multicollinearity according to Midi et al. (2010).

Multiple linear regression, a statistical technique, is utilized to predict the value of a dependent variable based on two or more independent variables. In this study, the multiple linear regression model was specified as: $Y = \beta_0 + \beta_1 X_1 + \beta_2 X_2 + \dots + \beta_n X_n + \epsilon$

where Y is the total number of strokes (both active and least-active lightning days), β_0 is the intercept, $\beta_1, \beta_2, \beta_3, \dots, \beta_n$ are the regression coefficients, $X_1, X_2, X_3, \dots, X_n$ are the independent variables (environmental predictors), ϵ is the error term.

While a multiple linear regression model captures the overall variation in stroke counts, it does not distinguish whether these environmental parameters are statistically significant in identifying active lightning days specifically. To address this, a logistic regression model was developed to classify the days as either active or least active based on four predictors.

The logistic regression model estimates the probability (p) of a binary outcome (i.e., an active or least-active lightning day) and is defined as:

$$p = \frac{1}{1 + e^{-z}}$$

where p is the probability of a day being active and z is a linear combination of predictors, expressed as:

$$z = \beta_0 + \beta_1 X_1 + \beta_2 X_2 + \dots + \beta_n X_n$$

where β_0 is the intercept, $\beta_1, \beta_2, \beta_3, \dots, \beta_n$ are the coefficients corresponding to the predictors $X_1, X_2, X_3, \dots, X_n$.

2.4.2. Principal component analysis

To explore the atmospheric differences between active and least-active lightning days, a Principal Component Analysis (PCA) was conducted using various thermodynamic and kinematic variables from soundings. Many Researchers (e.g., Rajeevan et al., 2012; Yadava et al., 2023; Kumar et al., 2024) used PCA to examine the relationships between lightning distribution and various meteorological, topographical, and thermodynamic factors around the world. PCA is a statistical technique used to reduce the dimensionality of a dataset and address potential multicollinearity among the independent variables. It transforms potentially correlated variables into a smaller set of uncorrelated variables, called principal components. Each principal component is orthogonal to the others and ranked according to the amount of variance it explains. The first principal component (PC1) accounts for the greatest variance, followed by the second (PC2), and so on. Typically, only the first few components are retained to capture most of the variance in the data. In PCA, eigenvalues represent the magnitude of the variance explained by each principal component, while eigenvectors represent the directions of those components. For further PCA methodological details, readers can refer to Jolliffe (2005) and Abdi and Williams (2010).

2.4.3. Box and whisker plot

Box and whisker plots were employed to visually analyze the distribution, central tendency, and variability of atmospheric variables associated with the most and least active lightning days. These plots graphically represent the five-number summary of a dataset: the minimum, first quartile (Q1), median (second quartile), third quartile (Q3), and maximum.

In each plot, a cross (\times) was used to denote the mean of the data. The central box represents the interquartile range (IQR), which extends from Q1 to Q3 and encompasses the middle 50 % of the data. The line inside the box indicates the median value. The "whiskers" extend to the smallest and largest values that fall within 1.5 times the IQR from the

respective quartiles. Data points outside this range are considered outliers and are plotted individually. Mathematically, these are defined as:

$$IQR = Q3 - Q1$$

$$\text{Lower bound} = Q1 - 1.5 \times IQR$$

$$\text{Upper bound} = Q3 + 1.5 \times IQR$$

3. Sounding comparisons

A wide variety of sounding parameters were calculated from the Dhaka radiosonde station at 00:00 UTC and 12:00 UTC for all active and least-active days. The average values of each parameter for both active and least-active cases were compared at both times. No significant differences were found; percentage differences between these two times were below 9 % for all parameters, except for SWI and SBCAPE, which showed differences of 38 % and 26 %, respectively. Consequently, comparisons of the studied parameters are presented in Figs. 2–4 only at 00:00 UTC (06:00 LST), as this time is more suitable for forecasting purposes. Morning data is critical for anticipating lightning activity later in the day.

The box and whisker plots in Figs. 2–4 display the distribution of 12 significant sounding parameters relevant to convection and storm severity. Fig. 2 includes temperature- and humidity-based indices. Fig. 3 focuses on humidity- and wind-related parameters, while Fig. 4 highlights thematic and advanced parameters. Definitions and threshold values for these parameters can be found in the AMS Glossary of Meteorology (<https://www.ametsoc.org/index.cfm/ams/publications/glossary-of-meteorology/>) and the National Weather Service (<https://www.weather.gov/forecast.weather.gov/glossary.php>).

Clear differences are observed between active and least-active lightning days across all parameters. Active days consistently exhibit greater atmospheric instability, stronger low-level wind shear, higher moisture content, and increased helicity compared to least-active days. The detailed analyses of these are below:

- (a) Total Totals Index (TTI): As shown in Fig. 2a, the TTI—representing the sum of the vertical and cross totals—indicates that thunderstorms are likely on active days with values ≥ 44 °C. In contrast, approximately 50 % of least-active days display a TTI of 37.6 °C, indicating a lower probability of thunderstorm development.
- (b) K Index (KI): Fig. 2b highlights that KI, which incorporates the temperature lapse rate, moisture content of the lower troposphere, and the vertical extent of the moist layer, suggests a 60 % to 90 % probability of thunderstorms occurring when KI ranges from 31 °C to over 40 °C on active days. Conversely, on least-active days, the probability of thunderstorm development drops to only 0–60 % with a KI below 30 °C.
- (c) Lifted Index (LI): Fig. 2c shows that LI, an indicator of atmospheric instability, is negative on almost all active days, signifying the likelihood of thunderstorms. In contrast, 50 % of the least-active days have positive LI values, suggesting a more stable atmosphere.
- (d) Equivalent Potential Temperature (θ_e): Fig. 2d illustrates that θ_e at LCL is significantly higher during active days, with an average of 350 K, compared to 336 K on least-active days. The maximum θ_e on active days is 366 K, compared to 358 K on least active days, indicating stronger vertical instability on active days.

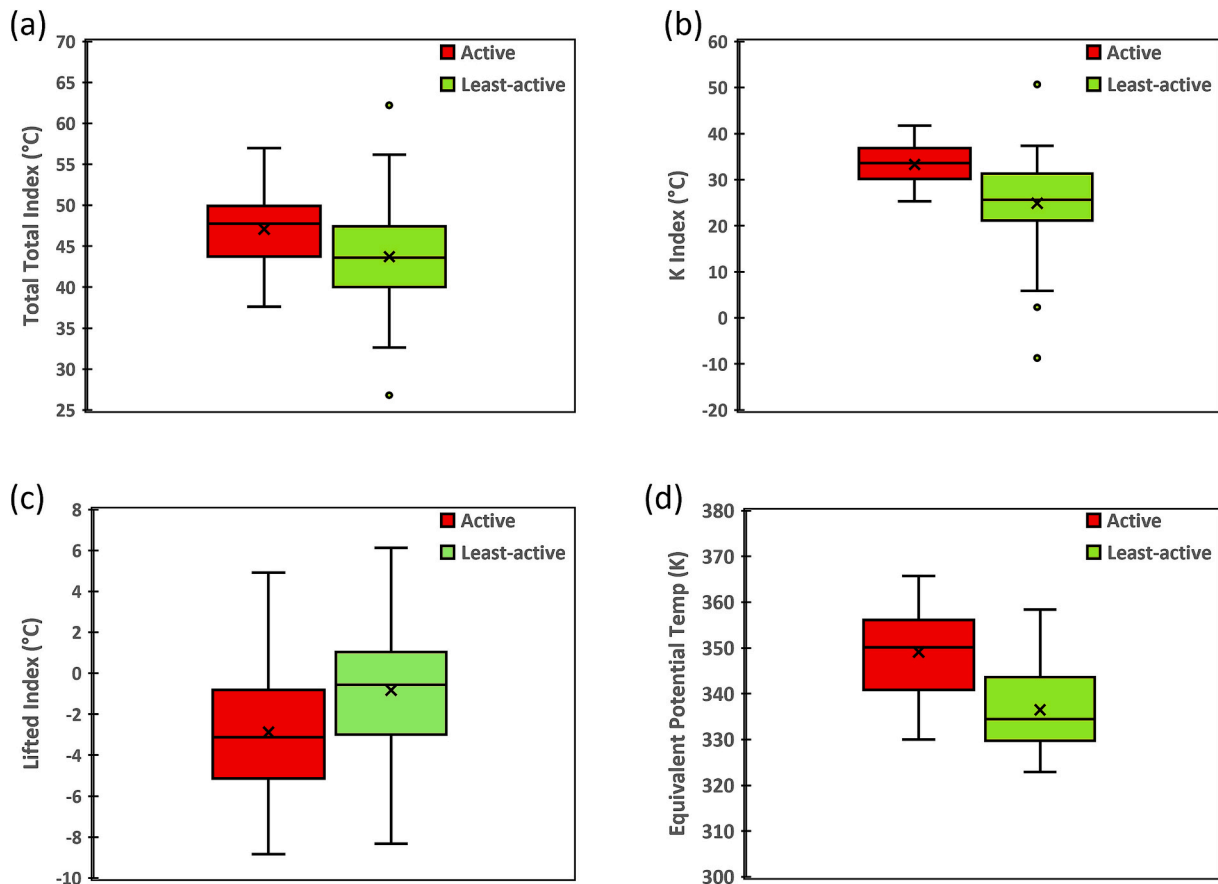


Fig. 2. Box and whisker plots showing various temperature and humidity-based indices calculated from upper air sounding at Dhaka, Bangladesh during 50 active, and 50 least-active lightning days (a) TTI, (b) KI, (c) LI, and (d) θ_e .

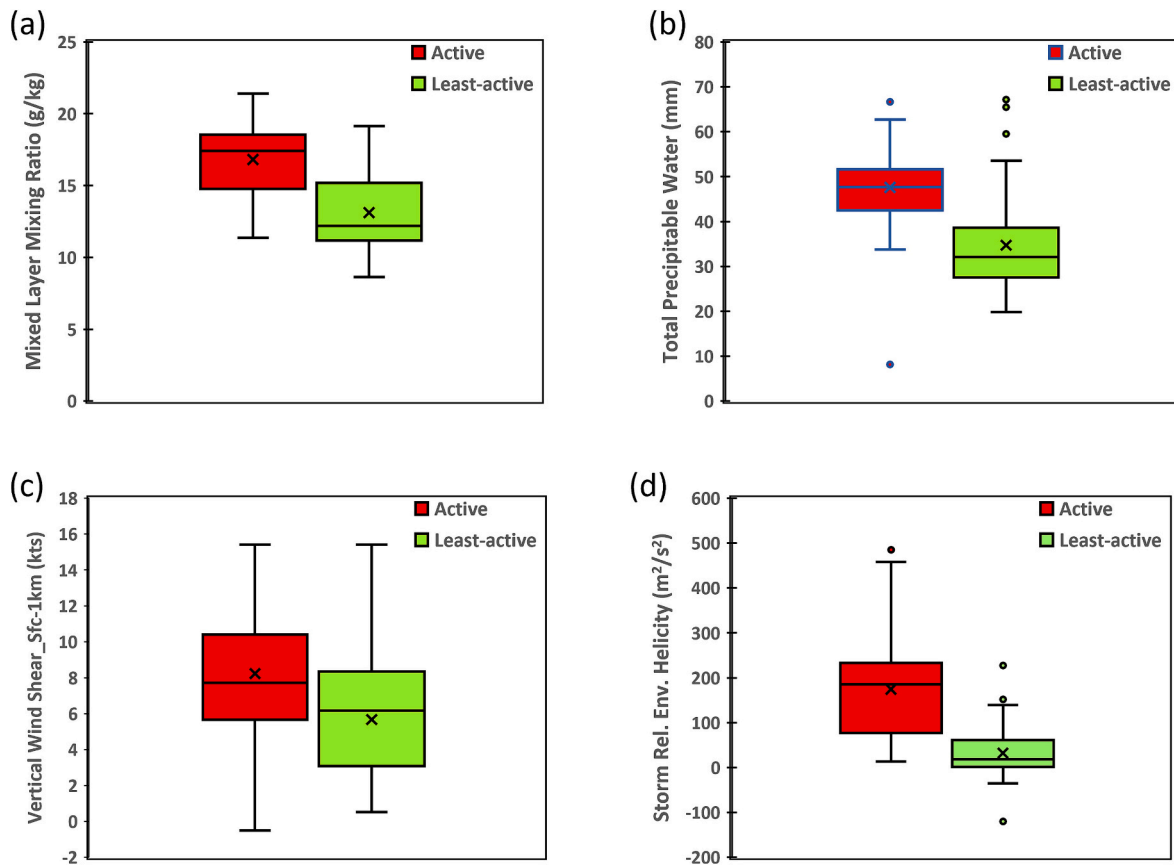


Fig. 3. Box and whisker plots illustrating various humidity and wind-related parameters calculated from upper air sounding at Dhaka, Bangladesh during 50 active, and 50 least-active lightning days (a) mixed layer Q, (b) TPW, (c) VWS from the surface to 1 km, and (d) SREH.

- (e) Mixed Layer Mixing Ratio (Q): Fig. 3a shows a negatively skewed distribution of the mixed layer mixing ratio on active days, while it is positively skewed on least-active days. Active days feature mixing ratios $>12 \text{ g kg}^{-1}$, reaching up to 21.4 g kg^{-1} , whereas half of the least-active days have a mixing ratio below 12 g kg^{-1} , with a maximum of 18.2 g kg^{-1} .
- (f) Total Precipitable Water (TPW): TPW is significantly higher on active days, with a maximum of 63 mm, compared to 53 mm on least-active days (Fig. 3b).
- (g) Vertical Wind Shear (VWS): The low-level VWS between the surface and 1 km is crucial for severe thunderstorms. Fig. 3c indicates that VWS values are generally higher on active days, with a maximum of 15.4 kts, suggesting the potential for strong thunderstorms.
- (h) Storm-Relative Environmental Helicity (SREH): More than 50 % of active days, SREH at 0–3 km values exceed $150 \text{ m}^2 \text{ s}^{-2}$, indicating thunderstorms with potential rotation (Fig. 3d). In 20 % of these cases, SREH values exceed $300 \text{ m}^2 \text{ s}^{-2}$, signaling the possibility of supercell thunderstorms and tornadoes. In the contrary situation, the least-active days typically exhibit thunderstorms with little or no rotation.
- (i) SWEAT Index: Fig. 4a demonstrates a sharp contrast between active and least-active days. The SWEAT index, which combines low-level moisture (850 hPa dewpoint), instability (TTI), lower and middle-level (850 and 500 hPa) wind speeds, and warm air advection (veering between 850 and 500 hPa) parameters, averages around 300 on active days but this index remains below 200 on most least-active days.
- (j) Lifting Condensation Level (LCL): Fig. 4b represents LCL, the cloud base height, which is lower on active days ($\sim 700 \text{ m}$, or 930 hPa) compared to least-active days ($\sim 1000 \text{ m}$, or 894 hPa).

- (k) SBCAPE and MUCAPE: Both SBCAPE and MUCAPE are depicted in the lower panels of Fig. 4 (c-d). CAPE serves as a measure of the available potential energy that fuels a thunderstorm. Higher values indicate greater potential for severe weather. MUCAPE represents CAPE of the most unstable parcel within the lowest 300 hPa. In Fig. 4 (c-d), the least-active days exhibit lower values for both CAPE parameters, with SBCAPE found to be $<1000 \text{ J kg}^{-1}$ and the maximum significant value for MUCAPE at 3266 J kg^{-1} . In contrast, within widely distributed CAPE values, 50 % of the cases on active days feature SBCAPE values of $>1000 \text{ J kg}^{-1}$, with the maximum MUCAPE value reaching 5628 J kg^{-1} .

4. Synoptic map comparisons

4.1. Environmental conditions during lightning events

During the pre-monsoon months, the northeastern Indian subcontinent, including Bangladesh, experiences Nor'westers and tornadoes (Yamane and Hayashi, 2006; Bikos et al., 2016). These phenomena are predominantly associated with arc-type squall line mesoscale convective systems (MCS) extending 100–300 km in length (Rafiuddin et al., 2010). Such severe pre-monsoon MCS events are primarily driven by the convergence of dry, hot northwesterly winds from arid regions and moist, warm southwesterly winds from the Bay of Bengal (BoB), forming a synoptic dryline along the eastern Indian coast and extending into Bangladesh (Aker and Tsuboki, 2017). Given the significant scale of these MCS, it is essential to examine the synoptic-scale environmental conditions in the study area.

Using ERA5 data, composite maps of key parameters in and around Bangladesh were developed for active versus least-active days. Figs. 5a-b depict the moisture flux (MF) and temperature anomalies averaging

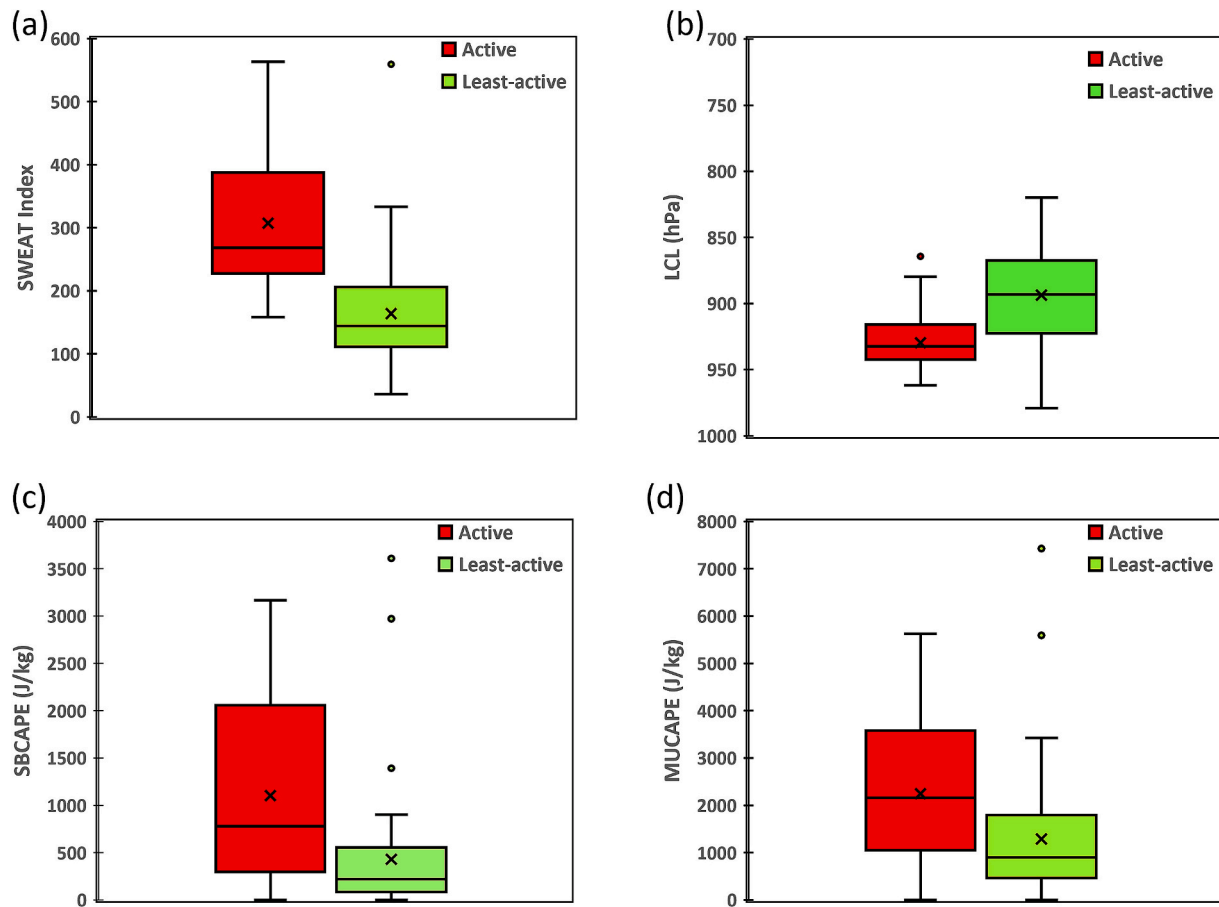


Fig. 4. Box and whisker plots showing various thematic and advanced parameters calculated from upper-air sounding at Dhaka, Bangladesh, during 50 active and 50 least-active lightning days (a) SWEAT index, (b) LCL, (c) SBCAPE, and (d) MUCAPE.

over the top 50 active and 50 least-active lightning days. A noticeably steeper temperature gradient (approximately 2 K within 100 km) is observed over Bangladesh on the active lightning days compared to the least-active days. In both scenarios, the moisture originates primarily from the southwest, reaching a maximum value of approximately $200 \text{ g m}^{-2} \text{ kg}^{-1}$ on active days and less than $100 \text{ g m}^{-2} \text{ kg}^{-1}$ on least-active days. The combination of sharp temperature gradients and elevated moisture levels plays a crucial role in the formation of intense thunderstorms.

Fig. 5c-d present 500 hPa wind vectors alongside the equivalent potential instability (PI), defined as the difference in equivalent potential temperature between 500 hPa and 850 hPa levels. These plots reveal significantly more unstable atmospheric conditions during active lightning days. Lower (more negative) PI values indicate greater instability. On active days, PI values over Bangladesh fall below -6 , whereas least-active days register positive values around 1 , indicating a much more stable atmosphere.

In summary, the areal averages of moisture and instability for the Bangladesh region ($87.3\text{--}92.8^\circ \text{ E}$, $20.6\text{--}26.9^\circ \text{ N}$) at 00:00 UTC were calculated for both active and least-active lightning cases. Active days exhibit an average MF of approximately $70 \text{ g m}^{-2} \text{ kg}^{-1}$, which decreases by over 35% in the least-active cases. The average PI value is around -4 on active days, compared to $+1$ on least-active days, highlighting the stark contrast in atmospheric stability between the two scenarios.

4.2. Hydrometeor conditions during lightning events

The separation of electrical charges that leads to lightning is heavily influenced by interactions among various hydrometeors within

thunderclouds under favorable environmental conditions. Strong updrafts within thunderstorms propel moisture and ice particles to higher altitudes, where collisions and charge separation occur. Simultaneously, downdrafts carry precipitation particles downward through the charging layer, further enhancing charge separation and eventually resulting in various forms of lightning discharges (Williams, 1985; Saunders, 1993). To investigate this mechanism, cloud ice water (CIW) content and cloud liquid water (CLW) content were analyzed at multiple vertical levels from 850 hPa to 200 hPa for both active and least-active lightning days, using ERA5 data. Additionally, vertical pressure velocity (ω) between 850 hPa and 200 hPa was examined to assess vertical air motion, both upward and downward.

On active days, significantly greater values of CIW and CLW were observed at 200 hPa and 850 hPa, respectively, compared to least-active days (Fig. 6). In Fig. 6a, CIW content is broadly distributed across Bangladesh, with a maximum average of approximately 0.055 g kg^{-1} at 200 hPa centered over the country. The negative ω between 850 hPa and 200 hPa layer indicates deep convection with stronger updrafts, accompanied by a maximum deep-layer ascent of -0.9 hPa s^{-1} . Similarly, Fig. 6c illustrates CLW content with a peak average value of approximately 0.2 g kg^{-1} at 850 hPa, along with a modest downward air motion of 0.5 hPa s^{-1} . In contrast, there is no notable presence of CIW or CLW content that is evident on the least-active days (Fig. 6b and d). Vertical air motion within the 850–200 hPa layer is also minimal, indicating a lack of deep convective activity over the region during those periods.

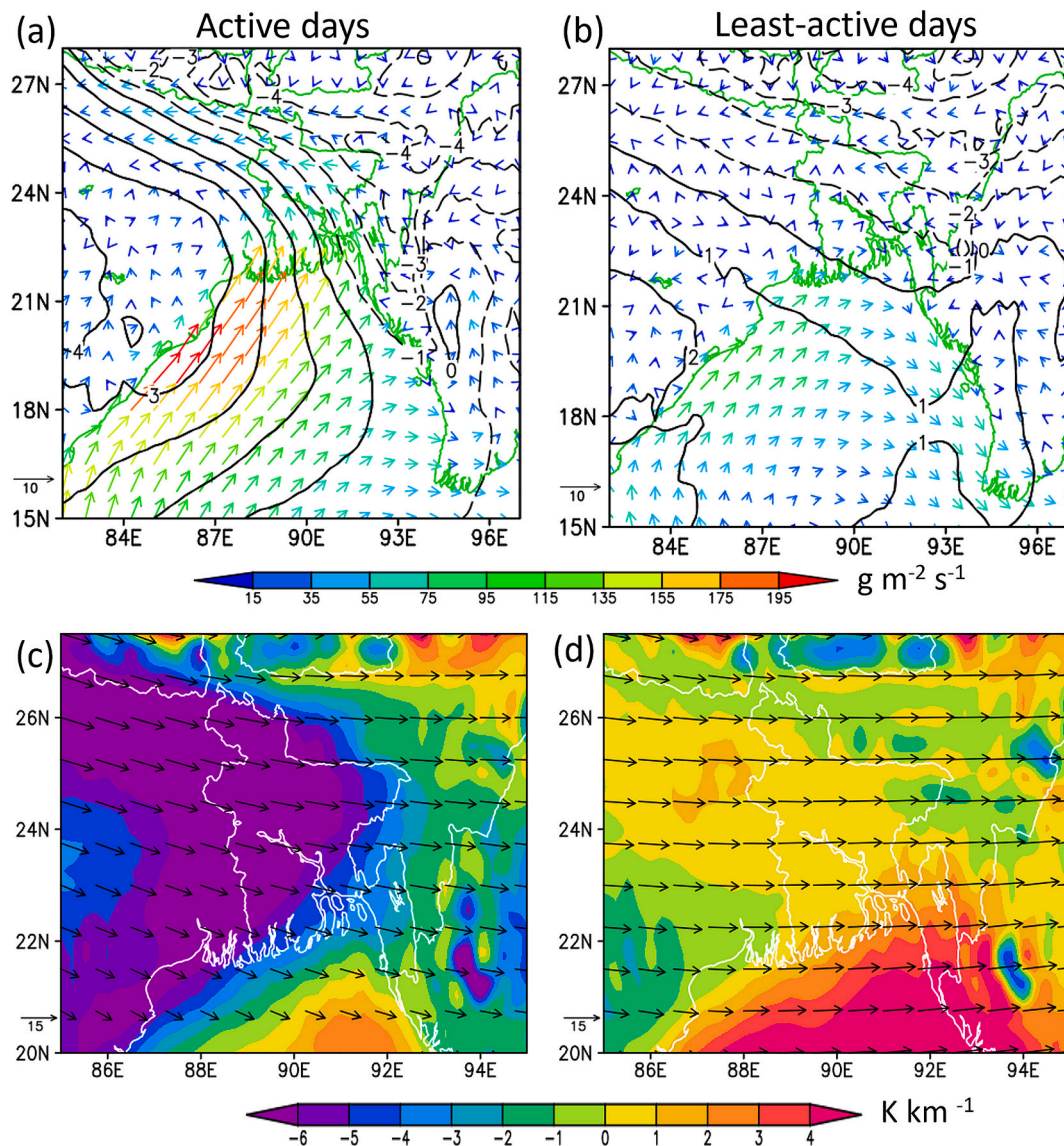


Fig. 5. Temperature anomalies at 850 hPa (contours; 1 K interval) calculated from the average area of background and surface wind velocity (vector; m s^{-1}) with moisture flux (color shaded in vector; $\text{g m}^{-2} \text{s}^{-1}$) for the average value of (a) active, and (b) least-active days. Equivalent potential temperature between 500 hPa and 850 hPa (shaded; K km^{-1}) and wind velocity (vector; m s^{-1}) at 500 hPa for the average value of (c) active, and (d) least-active days.

5. Discussion

5.1. Contribution of environmental parameters

The findings of this study highlight notable differences in synoptic-scale environmental conditions between active and least-active lightning days, particularly in terms of low-level moisture flux, temperature gradients, and potential instability. These variations are strongly associated with the presence of a pre-monsoon dryline over Bangladesh and the development of squall-line convection, including arc- or line-shaped MCS, which typically have a lifespan of approximately four hours (Rafiuddin et al., 2010). The surface dryline exhibits a mean diurnal oscillation of around 100 km from east to west (Akter and Tsuboki, 2017). The movement and intensity of this dry-moist boundary zone throughout the day are critical in modulating the daily variability and severity of convection, and by extension, lightning activity. Diurnal variations in hydrometeor characteristics, particularly CIW and CLW, are pronounced and closely tied to lightning occurrences. On active days, the average surface moisture flux over the Bangladesh region exceeded $60 \text{ g m}^{-2} \text{s}^{-1}$, while for 75 % of the least-active days (excluding

outliers), values remained below this threshold. Approximately 80 % of active days exhibited negative PI values, a clear contrast to the predominantly positive PI values observed on least-active days. Similarly, the areal average of CLW content at 850 hPa exceeded 0.01 g kg^{-1} on active days but fell below this value on least-active days. At 200 hPa, CIW content exceeded 0.002 g kg^{-1} on 80 % of active days, while it continued to be lower on least-active days. Table 1 shows a summary of the threshold limits for these synoptic-scale parameters.

Furthermore, for the relation between these four environmental parameters, i.e., MF, PI, CIW and CLW with lightning activity, statistical modeling was performed using both multiple linear regression and logistic regression (Table 2). Before modeling, multicollinearity among environmental predictors was assessed using VIF. The VIF values were found to range from 1.25 to 2.67, with a mean of 1.86 across the four predictors. While a VIF above 10 typically signals problematic multicollinearity, only CLW marginally exceeded the conservative threshold of 2.5, indicating generally acceptable levels of multicollinearity (Midi et al., 2010). The multiple linear regression model, incorporating four key environmental predictors, explained 60 % of the variability in lightning stroke counts ($R^2 = 0.60$). Among the predictors, PI ($p <$

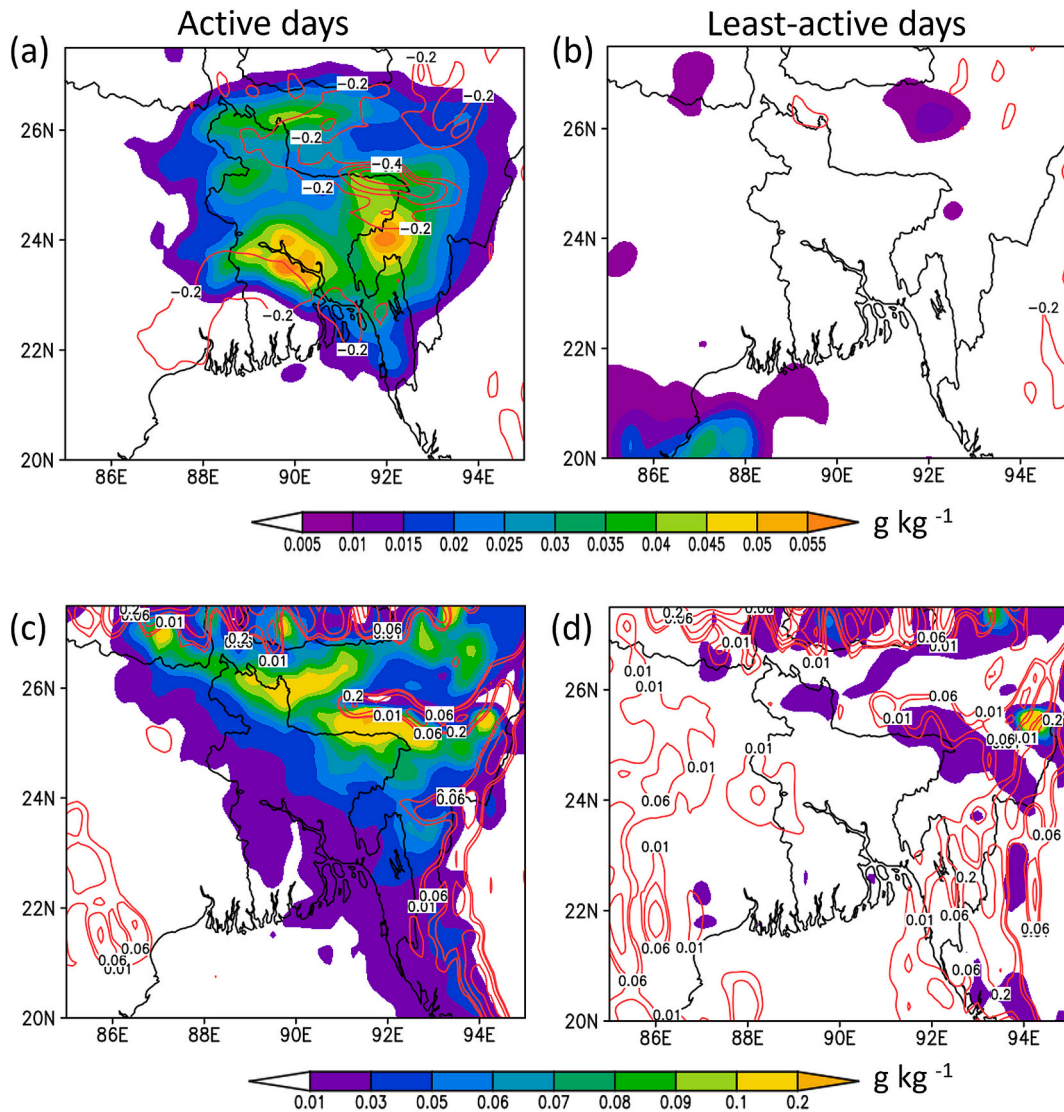


Fig. 6. Cloud ice water content (shaded; g kg^{-1}) and upward air motion between 850 hPa and 200 hPa (contours, hPa s^{-1}) averaged for (a) active, and (b) least-active days. Cloud liquid water content (shaded; g kg^{-1}) and downward air motion between 850 hPa and 200 hPa (contours, hPa s^{-1}) averaged for (c) active, and (d) least-active lightning days.

Table 1
Threshold values for various parameters between active and least-active lightning days.

Data	Parameters	Active lightning days	Least-active lightning days
Reanalysis	MF	$>60 \text{ g m}^{-2} \text{ s}^{-1}$	$<60 \text{ g m}^{-2} \text{ s}^{-1}$
	PI	Negative value	Positive value
	CIW	$>0.002 \text{ g kg}^{-1}$	$<0.002 \text{ g kg}^{-1}$
	CLW	$>0.01 \text{ g kg}^{-1}$	$<0.01 \text{ g kg}^{-1}$
	KI	$\geq 30 \text{ }^\circ\text{C}$	$< 30 \text{ }^\circ\text{C}$
	θ_e	$\geq 341 \text{ K}$	$< 341 \text{ K}$
	Q	$\geq 15 \text{ g kg}^{-1}$	$< 15 \text{ g kg}^{-1}$
Observed	TPW	$\geq 42 \text{ mm}$	$\leq 37 \text{ mm}$
	SREH	$\geq 65 \text{ m}^2 \text{ s}^{-2}$	$\leq 40 \text{ m}^2 \text{ s}^{-2}$
	SWEAT	≥ 230	≤ 200
	LCL	$\geq 918 \text{ hPa}$	$< 918 \text{ hPa}$
	SBCAPE	$\geq 460 \text{ J kg}^{-1}$	$\leq 380 \text{ J kg}^{-1}$
	MUCAPE	$\geq 1580 \text{ J kg}^{-1}$	$\leq 985 \text{ J kg}^{-1}$

0.001), CIW ($p < 0.001$), and CLW ($p < 0.001$) were statistically significant. PI showed a negative association with lightning strokes, while CIW and CLW were positively associated.

Complementing this, the logistic regression model classified days as

Table 2
Regression model analyses for various environmental parameters.

Regressions	Variables	Coefficient	Standard error	p-value
Multiple linear	Intercept	24,951.4	9720.0	0.012*
	PI	-5512.6	1264.1	3.28×10^{-5} ***
	MF	-209.9	215.8	0.33
	CIW	1,022,956.4	193,046.1	7.53×10^{-7} ***
	CLW	1,169,392.2	337,130.7	0.0008***
	Intercept	-2.82	0.94	0.003**
Logistic	PI	-0.57	0.16	0.0004***
	MF	-0.004	0.02	0.823
	CIW	70.84	40.98	0.08■
	CLW	111.01	39.74	0.005**

Significance codes: 0 ‘****’ 0.001 ‘***’ 0.01 ‘**’ 0.05 ‘*’ 0.1 ‘.’ 1.

either active or least active with a good degree of accuracy ($R^2 = 0.66$). In this model, PI ($p < 0.001$) and CLW ($p = 0.005$) were statistically significant predictors, while CIW was marginally significant ($p = 0.08$). As with the linear model, PI had a negative association with lightning activity, while CLW and CIW had positive associations.

Both models underscored the critical role of atmospheric instability,

as indicated by negative PI values, in initiating deep convection. In addition, the presence of upper-level cloud ice and low-level cloud water significantly contributes to lightning development. Notably, MF did not emerge as a statistically significant predictor in either model. However, θ_e , which is inherently linked to PI as it incorporates both temperature and moisture (<https://glossary.ametsoc.org/>), serves as an important proxy. Increased low-level moisture influx elevates θ_e , thereby intensifying atmospheric instability and fostering conditions favorable to severe convection, and thus, lightning.

5.2. Contribution of sounding parameters

In addition to the synoptic-scale environment, cloud-scale thermodynamic and kinematic parameters were analyzed to understand the daily variations in lightning activity associated with thunderstorms. Results (Figs. 2–4) revealed that active lightning days are more conducive to the development of strong convection, with conditions occasionally favorable for supercells and tornado formation. In contrast, the least-active lightning days tended to exhibit weaker or less frequent thunderstorms.

Several key thunderstorm-related parameters—such as TT, KI, LI, θ_e , Q, TPW, low-level VWS, SREH, SWEAT, LCL, SBCAPE, and MUCAPE—showed significant reductions on least-active days. Specifically, these parameters are decreased by approximately 7 %, 25 %, 71 %, 4 %, 22 %, 27 %, 31 %, 81 %, 47 %, 4 %, 61 %, and 50 %, respectively, when compared to active lightning days.

For forecasting applications, establishing threshold values for these sounding parameters is critical for distinguishing days with high lightning potential from those with minimal activity. In this study, all parameters were evaluated at 00:00 UTC due to the availability of upper-air data, which may introduce slight limitations in the precision of the derived thresholds. Nevertheless, as shown in Figs. 2–4, the majority of active lightning days (top 75 %) and least active days (bottom 75 %) generally adhered to meaningful threshold limits summarized in Table 1. However, clear threshold separations were less evident for TTI, LI, and low-level VWS. Notably, on 20 % of active days, SREH value ranged from 300 to 485 $m^2 s^{-2}$, indicating a significant likelihood of supercell thunderstorms and intense lightning activity.

The threshold values identified in this study differ slightly from those

proposed by Tyagi et al. (2011) for pre-monsoon season thunderstorms over Kolkata, India, located roughly 400 km from Dhaka. This discrepancy is likely attributable to methodological differences; while the Kolkata study compared thunderstorm days to fair weather days, our analysis specifically compared active versus least-active lightning days. Furthermore, while Murugavel et al. (2014) reported no significant relationship between CAPE (specifically, SBCAPE) and lightning activity during the pre-monsoon season in India, our results indicate that SBCAPE and MUCAPE, in particular, play important roles in lightning generation.

To further explore the atmospheric differences between active and least-active lightning days, PCA was conducted in this study using the aforementioned thermodynamic and kinematic variables. In the context of lightning research, PCA has been applied in previous studies to identify dominant atmospheric patterns associated with lightning activity. For instance, Rajeevan et al. (2012) utilized PCA to cluster correlated predictors related to lightning occurrences over southeast India. More recently, Kumar et al. (2024) used PCA to examine the relationships between lightning distribution and various meteorological, topographical, and thermodynamic factors in Uttarakhand, India. Their results emphasized the influence of deep convection, driven by surface heating and buoyant air parcels, on enhanced lightning activity.

To better understand the relationships among these variables, PCA was conducted, with results visualized through a biplot and contribution bar plots (Fig. 7). The first two principal components—PC1 (57.2 %) and PC2 (19.1 %)—together explained 76.3 % of the total variance. The PCA biplot (Fig. 7a), which overlays variable loadings (arrows) with event observations (points), showed a clear separation between active and least-active lightning days along PC1. Active days cluster on the positive side of PC1, while the least-active days fall on the negative side, indicating that the variables contributing most to PC1 play a dominant role in differentiating the two categories. From the direction and length of the arrows, active lightning days are strongly associated with elevated values of Q, θ_e , TPW, LCL, and MUCAPE. In contrast, the least-active days are not strongly aligned with any variables contributing to PC1. Fig. 7b quantifies the contribution of each variable to PC1, highlighting those exceeding the average (indicated by red dashed line) as the most influential.

PC2, which explains 19.1 % of the variance, served as a secondary

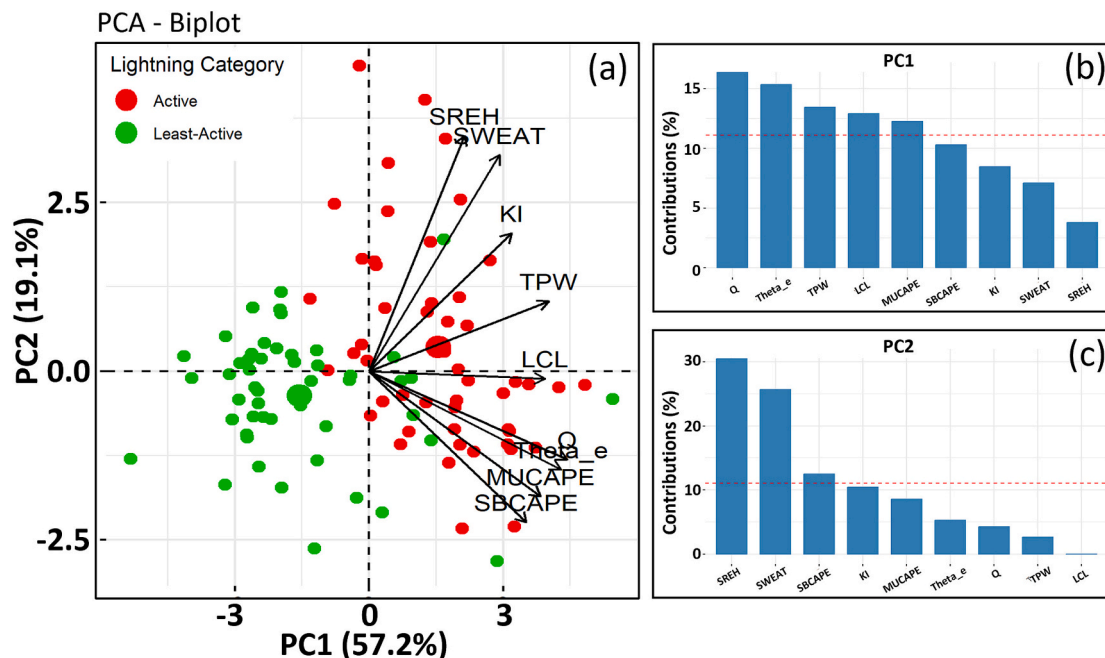


Fig. 7. (a) Biplot between PC1 and PC2, showing different variables for active and least-active lightning days. Contribution of variables to (b) PC1 and (c) PC2.

differentiator, mainly reflecting kinematic variables such as SREH and SWEAT, along with some influence from SBCAPE. In general, active lightning days are associated with diurnally increasing moisture, enhanced instability, and greater atmospheric energy, all of which favor deep convection and thunderstorm development compared to least-active days. These findings align well with the threshold-based analysis summarized in Table 1.

The daily variations in lightning activity can therefore be anticipated by monitoring increases in low-level moisture transport from the BoB, intensifying temperature gradients over Bangladesh, and the presence of unstable atmospheric conditions. Additionally, elevated amounts of high-level CIW and low-level CLW serve as key indicators of increased lightning potential. Similar observations have been reported by Dai et al. (2009) in China. Altogether, the synoptic-scale environment plays a significant role in modulating cloud-scale thermodynamic and kinematic parameters with meaningful threshold limits, ultimately driving lightning activity.

6. Conclusions

This study used GLD360 data from 2015 to 2020 to examine the differences in sounding profiles and synoptic-scale environments associated with the 50 most active and 50 least-active lightning days during the pre-monsoon season in Bangladesh. This season accounts for the majority of the lightning-related fatalities and injuries in the country, particularly among male agricultural workers. By analyzing 00:00 UTC (06:00 LST) radiosonde data from Dhaka along with ERA5 reanalysis data, several key thermodynamic and kinematic parameters were identified that effectively distinguish active from least-active lightning days over Bangladesh.

The synoptic-scale analysis revealed that active lightning days are consistently associated with enhanced low-level moisture flux, increased atmospheric instability (indicated by negative PI values), and higher concentrations of low-level CLW and high-level CIW. These conditions are often linked to the diurnal development and inland movement of the pre-monsoon dryline, which promotes convective organization, including squall lines and mesoscale convective systems. Regression analyses highlighted PI, CLW, and CIW as statistically significant and robust predictors of lightning activity.

KI, θ_e , Q, TPW, SREH, SWEAT, LCL, SBCAPE, and MUCAPE exhibited clear and consistent thresholds. Specifically, values below 30 °C, 341 K, 15 g kg⁻¹, 37 mm, 40 m² s⁻², 200, 918 hPa, 380 J kg⁻¹, and 985 J kg⁻¹ were commonly associated with least-active lightning days (1–500 strokes/day). In contrast, values exceeding these thresholds corresponded to a significantly increased likelihood of lightning activity, underscoring their predictive ability. PCA supported these findings, demonstrating clear atmospheric distinctions between active and least-active lightning days driven primarily by thermodynamic variables (Q, θ_e , TPW, LCL, and MUCAPE) and secondarily by kinematic factors (SREH and SWEAT). Notably, around 20 % of active days showed a potential for supercell thunderstorms and intense lightning activity, as they exhibited significantly higher SREH values exceeding 300 m² s⁻².

Collectively, these results demonstrated the feasibility of using early morning soundings from Dhaka, in conjunction with synoptic-scale environmental indicators, for operational forecasting of both extreme and non-extreme lightning events. Such forecasts could prove valuable in mitigating lightning-related risks, particularly for vulnerable populations to this localized hazard during the pre-monsoon season.

However, this study is not without limitations. First, radiosonde observations were only available from Dhaka, limiting spatial coverage across the country. Second, the spatial resolution of ERA5 dataset may be insufficient to resolve finer convective-scale features. Third, the absence of high-resolution cloud observations (e.g., weather radar data) constrained the analysis of detailed convective structures and evolution.

Despite these constraints, the findings offer a foundational understanding of the atmospheric conditions governing lightning activity in

Bangladesh, a data-scarce region vulnerable to various meteorological hazards. Future work should prioritize the integration of higher-resolution observational and modeling datasets and the expansion of national observational networks to enhance lightning prediction and early warning systems for at-risk communities.

CRedit authorship contribution statement

M. Rafiuddin: Writing – review & editing, Writing – original draft, Visualization, Software, Methodology, Formal analysis, Conceptualization. **Nasreen Akter:** Writing – review & editing, Writing – original draft, Visualization, Software, Methodology, Formal analysis, Conceptualization. **Ashraf Dewan:** Writing – review & editing, Writing – original draft, Validation, Supervision, Resources, Investigation, Data curation, Conceptualization. **Mohammed Sarfaraz Gani Adnan:** Writing – review & editing, Writing – original draft, Software, Resources, Investigation, Data curation. **Ronald L. Holle:** Writing – review & editing, Writing – original draft, Validation, Supervision, Methodology, Investigation, Data curation, Conceptualization.

Declaration of competing interest

The authors declare that they have no known competing financial interests or personal relationships that could have appeared to influence the work reported in this paper.

Acknowledgments

The authors are grateful to the Atmospheric Laboratory, Department of Physics, Bangladesh University of Engineering and Technology (BUET), Dhaka, for allowing the use of lab facilities. The authors also express their gratitude to all those involved with producing and disseminating the datasets used in this study. Special thanks are given to the anonymous reviewers for their valuable comments and suggestions, which have helped improve the quality of this paper. Mohammed Sarfaraz Gani Adnan acknowledges the Leverhulme Trust for the Early Career Fellowship.

Data availability

GLD360 data were provided by Vaisala Inc. Researchers can request access to GLD360 data through the Vaisala Research Data Grant Program through the following link: <https://www.vaisala.com/en/lp/request-vaisala-lightning-data-research-use>.

References

- Abdi, H., Williams, L.J., 2010. Principal component analysis. *Wiley Interdiscip. Rev. 2* (4), 433–459. <https://doi.org/10.1002/wics>.
- Akter, N., Tsuboki, K., 2017. Climatology of the premonsoon Indian dryline. *Int. J. Climatol.* 37 (11), 3991–3998. <https://doi.org/10.1002/joc.4968>.
- Albrecht, R.L., Goodman, S.J., Buechler, D.E., Blakeslee, R.J., Christian, H.J., 2016. Where are the lightning hotspots on Earth? *Bull. Am. Meteorol. Soc.* 97 (11), 2051–2068. <https://doi.org/10.1175/BAMS-D-14-00193.1>.
- Bikos, D., Finch, J., Case, J.L., 2016. The environment associated with significant tornadoes in Bangladesh. *Atmos. Res.* 167, 183–195. <https://doi.org/10.1016/j.atmosres.2015.08.002>.
- Case, J.L., Gatlin, P.N., Srikishen, J., Adhikary, B., Mannan, M.A., Bell, J.R., 2023. Building thunderstorm resilience in the Hindu Kush Himalaya Region through probabilistic forecasts and satellite observations. *Bull. Am. Meteorol. Soc.* 104 (5), E1105–E1131. <https://doi.org/10.1175/BAMS-D-21-0260.1>.
- Chandra, S., Siingh, D., Victor, N.J., Kamra, A.K., 2021. Lightning activity over South/Southeast Asia: Modulation by thermodynamics of lower atmosphere. *Atmos. Res.* 250, 105378. <https://doi.org/10.1016/j.atmosres.2020.105378>.
- Chowdhury, M.A.M., De, U.K., 1995. Pre-monsoon thunderstorm activity over Bangladesh from 1983 to 1992. *Terr. Atmos. Ocean. Sci.* 6 (4), 591–606. <https://doi.org/10.3319/TAO.1995.6.4.591A>.
- Christian, H.J., Blakeslee, R.J., Boccippio, D.J., Boeck, W.L., Buechler, D.E., Driscoll, K. T., Goodman, S.J., Hall, J.M., Koshak, W.J., Mach, D.M., Stewart, M.F., 2003. Global frequency and distribution of lightning as observed from space by the Optical Transient Detector. *J. Geophys. Res. Atmos.* 108 (D1). <https://doi.org/10.1029/2002JD002347> pp. ACL-4.

- Cooper, M.A., Holle, R.L., 2019. Reducing Lightning Injuries Worldwide. Springer International Publishing, New York, p. 233. <https://doi.org/10.1007/978-3-319-77563-0>.
- Dai, J., Wang, Y., Chen, L., Tao, L., Gu, J., Wang, J., Xu, X., Lin, H., Gu, Y., 2009. A comparison of lightning activity and convective indices over some monsoon-prone areas of China. *Atmos. Res.* 91 (2–4), 438–452. <https://doi.org/10.1016/j.atmosres.2008.08.002>.
- Dewan, A., Hossain, M.F., Rahman, M.M., Yamane, Y., Holle, R.L., 2017. Recent lightning-related fatalities and injuries in Bangladesh. *Weath. Clim. Soc.* 9 (3), 575–589. <https://doi.org/10.1175/WCAS-D-16-0128.1>.
- Dewan, A., Ongee, E.T., Rafiuddin, M., Rahman, M.M., Mahmood, R., 2018. Lightning activity associated with precipitation and CAPE over Bangladesh. *Int. J. Climatol.* 38 (4), 1649–1660. <https://doi.org/10.1002/joc.5286>.
- Dewan, A., Islam, K.A., Fariha, T.R., Murshed, M.M., Ishtiaque, A., Adnan, M.S.G., Kabir, Z., Chowdhury, M.B.H., 2022. Spatial pattern and land surface features associated with cloud-to-ground lightning in Bangladesh: an exploratory study. *Earth Syst. Environ.* 6 (2), 437–451. <https://doi.org/10.1007/s41748-022-00310-4>.
- Farukh, M.A., Islam, M.A., Uddin, M.N., 2023. Synoptic climatology of pre-monsoon frequent lightning events in Bangladesh. *Nat. Hazards* 116 (1), 1053–1070. <https://doi.org/10.1007/s11069-022-05711-2>.
- Gomes, C. (Ed.), 2021. *Lightning: Science, Engineering, and Economic Implications for Developing Countries*. Lecture Notes in Electrical Engineering, vol. 780. Springer Nature, 330 pp. ISBN:978-981-16-3439-0.
- Holle, R.L., 2016. A summary of recent national-scale lightning fatality studies. *Weath. Clim. Soc.* 8 (1), 35–42. <https://doi.org/10.1175/WCAS-D-15-0032.1>.
- Holle, R.L., Demetriades, N.W.S., Nag, A., 2016. Objective airport warnings over small areas using NLDN cloud and cloud-to-ground lightning data. *Weather Forecast.* 31, 1061–1069.
- Holle, R.L., Dewan, A., Said, R., Brooks, W.A., Hossain, M.F., Rafiuddin, M., 2019. Fatalities related to lightning occurrence and agriculture in Bangladesh. *Int. J. Disast. Risk Reduct.* 41, 101264. <https://doi.org/10.1016/j.ijdrr.2019.101264>.
- Jolliffe, I., 2005. *Principal Component Analysis*, 2nd edn. John Wiley & Sons Ltd. <https://doi.org/10.1002/0470013192> (BSA501).
- Kalashnikov, D.A., Davenport, F.V., Labe, Z.M., Loikith, P.C., Abatzoglou, J.T., Singh, D., 2024. Predicting cloud-to-ground lightning in the western United States from the large-scale environment using explainable neural networks. *J. Geophys. Res. Atmos.* 129 (22), e2024JD042147. <https://doi.org/10.1029/2024JD042147>.
- Kandalgaonkar, S.S., Tinmaker, M.I.R., Kulkarni, J.R., Nath, A., 2003. Diurnal variation of lightning activity over the Indian region. *Geophys. Res. Lett.* 30 (20). <https://doi.org/10.1029/2003GL018005>.
- Kodama, Y.M., Ohta, A., Katsumata, M., Mori, S., Satoh, S., Ueda, H., 2005. Seasonal transition of predominant precipitation type and lightning activity over tropical monsoon areas derived from TRMM observations. *Geophys. Res. Lett.* 32 (14). <https://doi.org/10.1029/2005GL022986>.
- Kumar, S., Gautam, A.S., Kamra, A.K., Singh, K., Potdar, S.S., Siingh, D., 2024. Lightning distribution and its association with surface thermodynamics parameters over a western Himalayan region. *J. Earth Syst. Sci.* 133 (4), 234. <https://doi.org/10.1007/s12040-024-02406-z>.
- Li, J., Wu, X., Yang, J., Jiang, R., Yuan, T., Lu, J., Sun, M., 2020. Lightning activity and its association with surface thermodynamics over the Tibetan Plateau. *Atmos. Res.* 245, 105118. <https://doi.org/10.1016/j.atmosres.2020.105118>.
- Medina, S., Houze Jr., R.A., Kumar, A., Niyogi, D., 2010. Summer monsoon convection in the Himalayan region: Terrain and land cover effects. *Q. J. R. Meteorol. Soc.* 136 (648), 593–616. <https://doi.org/10.1002/qj.601>.
- Midi, H., Sarkar, S.K., Rana, S., 2010. Collinearity diagnostics of binary logistic regression model. *J. Interdiscip. Math.* 13 (3), 253–267. <https://doi.org/10.1080/09720502.2010.10700699>.
- Ministry of Disaster Management and Relief (MoDMR), 2019. *Standing orders on disasters 2019*. Government of Bangladesh, Dhaka.
- Murugavel, P., Pawar, S.D., Gopalakrishnan, V., 2014. Climatology of lightning over Indian region and its relationship with convective available potential energy. *Int. J. Climatol.* 34 (11). <https://doi.org/10.1002/joc.3901>.
- Nag, A., Holle, R.L., Murphy, M.J., 2017. *Lightning: Cloud-to-ground lightning over the Indian subcontinent*. In: *Postprints of the 8th Conference on the Meteorological Applications of Lightning Data*. American Meteorological Society, Seattle/Washington, pp. 22–26.
- Paul, P., Imran, A., Mallik, M.A.K., Syed, I.M., 2022. Diagnostic study of the lightning potential index and electric field in two thunderstorm cases over Bangladesh. *Atmos. Ocean Opt.* 35 (5), 524–540. <https://doi.org/10.1134/S1024856022050177>.
- Qie, K., Qie, X., Tian, W., 2021. Increasing trend of lightning activity in the South Asia region. *Sci. Bull.* 66 (1), 78–84. <https://doi.org/10.1016/j.scib.2020.08.033>.
- Rabbani, K.M.G., Islam, M.J., Fierro, A.O., Mansell, E.R., Paul, P., 2022. Lightning forecasting in Bangladesh based on the lightning potential index and the electric potential. *Atmos. Res.* 267, 105973. <https://doi.org/10.1016/j.atmosres.2021.105973>.
- Rafiuddin, M., Uyeda, H., Islam, M.N., 2010. Characteristics of monsoon precipitation systems in and around Bangladesh. *Int. J. Climatol.* 30 (7), 1042–1055. <https://doi.org/10.1002/joc.1949>.
- Rajeevan, M., Madhulatha, A., Rajasekhar, M., Bhat, J., Kesarkar, A., Rao, B.A., 2012. Development of a perfect prognosis probabilistic model for prediction of lightning over south-East India. *J. Earth Syst. Sci.* 121, 355–371. <https://doi.org/10.1007/s12040-012-0173-y>.
- Romatschke, U., Houze Jr., R.A., 2011. Characteristics of precipitating convective systems in the premonsoon season of South Asia. *J. Hydrometeorol.* 12 (2), 157–180. <https://doi.org/10.1175/2010JHM1311.1>.
- Romatschke, U., Medina, S., Houze Jr., R.A., 2010. Regional, seasonal, and diurnal variations of extreme convection in the south Asian region. *J. Clim.* 23 (2), 419–439. <https://doi.org/10.1175/2009JCLI3140.1>.
- Sahu, R.K., Dadich, J., Tyagi, B., Vissa, N.K., Singh, J., 2020. Evaluating the impact of climate change in threshold values of thermodynamic indices during pre-monsoon thunderstorm season over Eastern India. *Nat. Hazards* 102, 1541–1569. <https://doi.org/10.1007/s11069-020-03978-x>.
- Said, R., 2017. Towards a global lightning locating system. *Weather* 72 (2). <https://doi.org/10.1002/wea.2952>.
- Said, R.K., Inan, U.S., Cummins, K.L., 2010. Long-range lightning geolocation using a VLF radio atmospheric waveform bank. *J. Geophys. Res. Atmos.* 115 (D23). <https://doi.org/10.1029/2010JD013863>.
- Said, R.K., Cohen, M.B., Inan, U.S., 2013. Highly intense lightning over the oceans: Estimated peak currents from global GLD360 observations. *J. Geophys. Res.-Atmos.* 118 (13), 6905–6915. <https://doi.org/10.1002/jgrd.50508>.
- Said, R., Golkowski, M., Harid, V., 2023. Empirical parameterization of broadband VLF attenuation in the Earth-Ionosphere waveguide. *J. Geophys. Res.* 128 (4), e2022JA030742. <https://doi.org/10.1029/2022JA030742>.
- Saunders, C.P.R., 1993. A review of thunderstorm electrification processes. *J. Appl. Meteorol. Climatol.* 32 (4), 642–655. <https://www.jstor.org/stable/45405622>.
- Siingh, D., Kumar, P.R., Kulkarni, M.N., Singh, R.P., Singh, A.K., 2013. Lightning, convective rain and solar activity—over the South/Southeast Asia. *Atmos. Res.* 120, 99–111. <https://doi.org/10.1016/j.atmosres.2012.07.026>.
- Siingh, D., Buchunde, P.S., Singh, R.P., Nath, A., Kumar, S., Ghodpage, R.N., 2014. Lightning and convective rain study in different parts of India. *Atmos. Res.* 137, 35–48. <https://doi.org/10.1016/j.atmosres.2013.09.018>.
- Sugimoto, S., Takahashi, H.G., 2017. Seasonal differences in precipitation sensitivity to soil moisture in Bangladesh and surrounding regions. *J. Clim.* 30 (3), 921–938. <https://doi.org/10.1175/JCLI-D-15-0800.1>.
- Suriano, Z.J., Loewy, C., Uz, J., 2023. Synoptic climatology of central US snowfall. *J. Appl. Meteorol. Climatol.* 62 (12), 1731–1743. <https://doi.org/10.1175/JAMC-D-23-0097.1>.
- Tyagi, B., Nareish Krishna, V., Satyanarayana, A.N.V., 2011. Study of thermodynamic indices in forecasting pre-monsoon thunderstorms over Kolkata during STORM pilot phase 2006–2008. *Nat. Hazards* 56, 681–698. <https://doi.org/10.1007/s11069-010-9582-x>.
- Umakanth, N., Satyanarayana, G.C., Simon, B., Rao, M.C., Babu, N.R., 2020. Analysis of lightning flashes over Bangladesh. In: *AIP Conference Proceedings*, vol. 2220. AIP Publishing. <https://doi.org/10.1063/5.0001294>. No. 1.
- Uman, M.A., 2009. *The Art and Science of Lightning Protection*. Cambridge University Press, p. 256. ISBN-13:9780521158251. <https://doi.org/10.1017/CBO9780511585890>.
- Virts, K.S., Lang, T.J., Buechler, D.E., Bitzer, P.M., 2024. Bayesian analysis of the detection performance of the lightning imaging sensors. *J. Atmos. Ocean. Technol.* 41 (5), 441–455. <https://doi.org/10.1175/JTECH-D-23-0090.1>.
- Walsh, K.M., Cooper, M.A., Holle, R., Rakov, V.A., Roeder, W.P., Ryan, M., 2013. National Athletic Trainers' Association position statement: lightning safety for athletics and recreation. *J. Athl. Train.* 48 (2), 258–270. <https://doi.org/10.4085/1062-6050-48.2.25>.
- Watson, A.I., Holle, R.L., López, R.E., 1994. Cloud-to-ground lightning and upper-air patterns during bursts and breaks in the southwest monsoon. *Mon. Weather Rev.* 122 (8), 1726–1739. [https://doi.org/10.1175/1520-0493\(1994\)122%3C1726:CTGLAU%3E2.0.CO;2](https://doi.org/10.1175/1520-0493(1994)122%3C1726:CTGLAU%3E2.0.CO;2).
- Weston, K.J., 1972. The dry-line of Northern India and its role in cumulonimbus convection. *Q. J. R. Meteorol. Soc.* 98 (417), 519–531. <https://doi.org/10.1002/qj.49709841704>.
- Williams, E.R., 1985. Large-scale charge separation in thunderclouds. *J. Geophys. Res. Atmos.* 90 (D4), 6013–6025. <https://doi.org/10.1029/JD090iD04p06013>.
- Yadava, P.K., Sharma, A., Payra, S., Mall, R.K., Verma, S., 2023. Influence of meteorological parameters on lightning flashes over Indian region. *J. Earth Syst. Sci.* 132 (4), 179. <https://doi.org/10.1007/s12040-023-02188-w>.
- Yamane, Y., Hayashi, T., 2006. Evaluation of environmental conditions for the formation of severe local storms across the Indian subcontinent. *Geophys. Res. Lett.* 33 (17). <https://doi.org/10.1029/2006GL026823>.